Experimental Cell Research 386 (2020) 111706

Contents lists available at ScienceDirect

Experimental Cell Research

journal homepage: www.elsevier.com/locate/yexcr

Krüppel-like factor 15 is a key suppressor of podocyte fibrosis under rotational force-driven pressure

Mi-Yeon Yu[a,1], Ji Eun Kim[b,1], Saram Lee[c], Jin Woo Choi[d], Yong Chul Kim[b], Seung Seok Han[b], Hajeong Lee[b,h], Ran Hui Cha[e], Jung Pyo Lee[f], Jae Wook Lee[g], Dong Ki Kim[b,h], Yon Su Kim[b,h], Seung Hee Yang[c,h,*]

[a] Department of Internal Medicine, Hanyang University Guri Hospital, Republic of Korea
[b] Department of Internal Medicine, Seoul National University Hospital, Seoul, Republic of Korea
[c] Seoul National University Hospital Biomedical Research Institute, Seoul, Republic of Korea
[d] Interdisciplinary Program in Bioengineering Major, Graduate School, Seoul National University, Seoul, Republic of Korea
[e] Department of Internal Medicine, National Medical Center, Seoul, Republic of Korea
[f] Department of Internal Medicine, Seoul National University Boramae Medical Center, Seoul, Republic of Korea
[g] Nephrology Clinic, National Cancer Center, Goyang, Gyeonggi-do, Republic of Korea
[h] Kidney Research Institute, Seoul National University College of Medicine, Seoul, Republic of Korea

ARTICLE INFO

Keywords:
KLF15
Podocyte
Chronic kidney disease
Hypertension
Rotational force
Nephropathy

ABSTRACT

Krüppel-like factor 15 (KLF15) is a well-known transcription factor associated with podocyte injury and fibrosis. Recently, hypertensive nephropathy was discovered to be closely related to podocyte injury and fibrosis. However, methods to stimulate hypertension *in vitro* are lacking. Here, we constructed an *in vitro* model mimicking hypertension using a rotational force device to identify the role of KLF15 in fibrosis due to mechanically induced hypertensive injury. First, we found that KLF15 expression was decreased in patients with hypertensive nephropathy. Then, an *in vitro* study of hypertension due to rotational force was conducted, and an increase in fibrosis markers and decrease in KLF15 levels were determined after application of 4 mmHg pressure in primary cultured human podocytes. KLF15 and tight junction protein levels increased with retinoic acid treatment. siRNA-mediated inhibition of *KLF15* exacerbated pressure-induced fibrosis injury, and KLF15 expression after treatment with angiotensin II was similar to that observed after treatment with the blood pressure modeling device. Furthermore, the reduced KLF15 levels after mechanical pressure application were restored after the administration of an antihypertensive drug. KLF15 expression was also low *in vivo*. We confirmed the protective role of KLF15 in fibrosis using a mechanically induced *in vitro* model of hypertensive injury.

1. Introduction

Krüppel-like factors (KLFs), a group of transcription factors, regulate diverse biological processes, including cell proliferation, differentiation, metabolism, inflammation, and survival [1]. Among the KLF family members, KLF15 is enriched in the kidney and liver and is a critical regulator of podocyte differentiation and renal fibrosis [2]. In past studies, the protective effects of KLF15 against fibrosis have been identified in experiments using angiotensin II-treated cells and mice and 5/6 nephrectomized rats [3–5]. Furthermore, a recent study showed that KLF15 binds to the promoter regions of genes encoding nephrin and podocin, which are podocyte differentiation markers induced by retinoic acid (RA) [6].

Hypertension is the second most common cause of end-stage renal disease [7–9], and the pathophysiology of hypertensive nephropathy has recently been discovered to be closely related to podocyte damage and the accumulation of fibrosis factors [10,11], as well as nephroangiosclerosis and arterial hyalinosis in the capillary tuft [12,13]. Most *in vitro* studies on hypertensive nephropathy or renal fibrosis have focused on angiotensin II-mediated activation of the renin-angiotensin system (RAS) or TGF-β-mediated induction of fibrosis in cell lines [14–17] Although chemical agents such as angiotensin II and TGF-β effectively induce fibrosis, this direct induction does not represent the complete series of dynamic processes associated with fibrosis, inflammation, and apoptosis following various renal injuries *in vivo*. In fact, to date, no specific disease model has been created solely using a

* Corresponding author. Kidney Research Institute, Seoul National University, 101 Daehakro Jongno-gu, Seoul, 110-744, Republic of Korea.
E-mail address: ysh5794@gmail.com (S.H. Yang).
[1] Both authors equally contributed to this work.

https://doi.org/10.1016/j.yexcr.2019.111706
Received 20 September 2019; Received in revised form 28 October 2019; Accepted 30 October 2019
Available online 04 November 2019

cell culture device. To this point, we attempted to establish an ideal *in vitro* disease model by creating an environment similar to hypertensive conditions using only rotational force with cultured cells. In addition, using this mechanical injury model, we tried to elucidate how KLF15, which was previously found to be associated with fibrosis and podocyte differentiation, affects podocytes based on actual pressure-induced stress rather than chemical injury. The aim of the present study, therefore, was to investigate the effect of KLF15 on podocytes and renal tissue in a newly developed mechanical hypertensive injury model to determine whether KLF15 can be used as a potential treatment target for hypertensive nephropathy.

2. Materials and methods

2.1. Assessment of podocyte fibrosis in biopsy-proven hypertensive nephropathy

The Institutional Review Board of the Seoul National University Hospital reviewed and approved the protocols for obtaining kidney biopsy tissues from patients with hypertensive nephropathy, IgA nephropathy, and normal kidneys (IRB no. H-1607-133-777). Patients with hypertensive nephropathy (n = 9), IgA nephropathy as disease controls (n = 7), and normal kidneys as healthy controls were subjected to ultrasonography-guided percutaneous needle biopsy. Hypertensive nephropathy was diagnosed based on typical pathological findings based on renal biopsy and uncontrolled blood pressure. IgA nephropathy was diagnosed based on renal biopsy revealing the presence of IgA-dominant or co-dominant immune deposits within glomeruli. Normal kidneys were diagnosed based on nonspecific findings in the glomeruli or tubules. KLF15 expression was visualized using immunofluorescence staining with a confocal microscope (Leica TCS SP8 STED CW instrument, Mannheim, Germany). The number of KLF15-positive cells was assessed for quantitative analysis. The clinical information for the patients, including age, sex, systolic blood pressure, diastolic blood pressure, spot urine protein/creatinine ratio, spot urine red blood cell counts, estimated glomerular filtration rate, and history of hypertension was obtained upon reviewing the electronic medical charts.

2.2. Human primary podocyte preparation

Human primary podocytes were harvested and cultured, as mentioned in our previous studies [18,19]. Briefly, kidney specimens were surgically resected from patients diagnosed with renal cell carcinoma, and the kidney cortices were mechanically dissected. The cortices were sieved to isolate the glomeruli, which were cultured for 8 days. The outgrowing cells were trypsinized and passed through sieves with a 25-μm pore size to obtain mesangial cells without the remaining glomerular cores. As these cells consist of podocytes, mesangial cells, and endothelial cells, they were sorted using flow cytometry to isolate podocytes. On day 8, the cultured cells were enumerated, and 1×10^6 cells were incubated with Fc receptor blocking reagent (1 μg/mL, BD Bioscience, San Jose, CA, USA). To identify the podocytes, the cells were stained with rabbit anti-human purified *anti*-podocalyxin (Abcam, Cambridge, UK) and fluorescein isothiocyanate-labeled anti-rabbit IgG (BD PharMingen, San Jose, CA, USA). Phycoerythrin-conjugated anti-CD90 (BD Pharmingen) and anti-CD31 (BD Pharmingen) were used to detect mesangial cells and glomerular endothelial cells, respectively. The stained cells were sorted and analyzed using a fluorescence-activated cell sorting (FACS) Calibur instrument (BD Biosciences). The homogeneous podocytes were further cultured in an incubator at 37 °C in a humid 5% CO_2 atmosphere.

Dulbecco's modified Eagle's medium (DMEM)/F12 (Lonza, Basel, Switzerland) supplemented with 15% fetal bovine serum (Gibco, Grand Island, NY, USA), 1 × insulin-transferrin-selenium (Gibco), 1 mM HEPES buffer (Sigma-Aldrich, St. Louis, MO, USA), 200 μM L-glutamine (Gibco), 50 nM hydrocortisone (Sigma-Aldrich), 100 U/mL penicillin (Gibco), and 100 pg/mL streptomycin (Gibco) was used to culture the podocytes, and the medium was changed after every 3 days. To determine the optimal media, the medium was supplemented in some experiments with 2% or 15% fetal bovine serum. Cells were plated on plastic dishes coated with 10 μg/mL fibronectin (Sigma-Aldrich) using standard methods. Depending on the exact experimental setup, RA (0.5 and 1 μmol/L, Santa Cruz Biotechnology, Santa Cruz, CA, USA), angiotensin II (1 μmol/L, Sigma-Aldrich), and losartan (0.1, 1, and 10 μmol/L, Sigma-Aldrich) were also added.

2.3. Pressurizing devices: design and manufacturing

This device, based on the design of the centrifuge, was constructed to apply sustained pressure on the cultured cells. The device consists of a main body, mounting docks, motor, and control unit. The main body (axis) and mounting dock of the device were made of an aluminum alloy and Teflon, respectively, using a lathe and milling machine. The dimensions of the device were 370 mm (width) × 370 mm (length) × 400 mm (height). The weight of the device was approximately 8 kg. The mounting dock can be used for various commercialized cell culture units such as a 100-pie dish or 6-well dish and allows for the cultivation of cells in large quantities. The motor was a brushless DC motor (BL42S-24026N-IG43, D&J WITH Co. Ltd., Seoul, Korea) with a 1/17 gear ratio. The revolutions per minute ranged from 0 to 235, and the rated torque was 7 kgf-cm. The control unit adjusted the motor speed and display based on the microcontroller (Arduino, Italy). The pressure applied to the cells could be controlled by changing the rate of revolutions per minute. The pressure applied to the cell dish according to the revolutions per minute was measured using a digital pressure transmitter (PSHHC1000HCPG, Sensys Inc.).

2.4. Fibrosis induction in human primary podocytes with a pressurizing device

For the induction of fibrosis, human primary podocytes were cultured in 6-well culture plates (1×10^5 cells/well), and four culture plates were mounted on the proposed pressuring system for the experiments. The pressuring system was placed inside a 5% CO_2 incubator at 37 °C during the experiments. Different time and pressure conditions were evaluated to determine the most suitable condition for the induction of fibrosis. Three different operating times were tested as follows: 3 h for short, 48 h for intermediate, and 72 h for long durations. Three different operating pressures were assessed, namely, static, 4 mmHg, and 8 mmHg. After the induction of fibrosis using the device, the methods to assess podocyte fibrosis and further analysis were as follows.

2.4.1. Quantitative reverse-transcription polymerase chain reaction (qRT-PCR)

Total RNA was extracted from the cells, and the mRNA levels of the target genes were assayed by qRT- PCR. Briefly, total RNA was extracted from the primary cultured podocytes using the RNeasy kit (Qiagen GmbH, Hilden, Germany), and 500 ng total RNA was reverse-transcribed using oligo-d(T) primers and AMV-RT Taq polymerase (Promega, Madison, WI, USA). qRT- PCR was performed using either Assay-on-Demand TaqMan probes or the SYBR Green method and primers for *FN1* (fibronectin), *PODXL* (podocalyxin), *WT-1* (Wilms' tumor), *KLF15*, and *GAPDH* (Applied Biosystems, Foster City, CA, USA), and analyzed using the Applied Biosystems PRISM 7500 sequence detection system. Relative quantification was performed using the $2^{-\Delta\Delta CT}$ method [20]. *GAPDH* was used as a loading control, and mRNA expression levels were normalized to *GAPDH* mRNA expression. All experiments were performed in triplicate. PCR primers used for qRT-PCR are listed in Table 1.

Table 1
Primer sets used for qRT-PCR.

Genes	Sequence (5′-3′) F	Sequence (5′-3′) R
FN1	CCACCCCCATAAGGCATAGG	GTAGGGGTCAAAGCACGAGTCATC
PODXL	GAGCAGTCAAAGCCACCTTC	TGGTCCCCTAGCTTCATGTC
WT-1	GAAAATAGGGGATGGTCCAG	CAATGGATTTCCTCACCCAG
KLF15	CAAAAGCAGCCACCTCAAG	TCTTCTCGCACACAGGACAC
GAPDH	TCGACAGTCAGCCGCATCT	CCGTTGACTCCGACCTTCA

Abbreviation: qRT-PCR, quantitative reverse transcription polymerase chain reaction.

2.4.2. Western blot analysis

Protein was extracted from the cells using radioimmunoprecipitation assay (RIPA) buffer containing the Halt protease inhibitor (Pierce, Rockford, IL, USA). Western immunoblotting was performed using primary antibodies against fibronectin (Abcam, Cambridge, MA), WT-1 (Abcam), KLF15 (Abcam), zonula occludens-1 (ZO-1) (Abcam), and β-actin (Sigma-Aldrich). Briefly, equal amounts (40 μg) of the extracted proteins were separated on 10% sodium dodecyl sulfate-polyacrylamide gels and transferred onto Immobilon-FL 0.4 μM polyvinylidene difluoride membranes (Millipore, Billerica, MA, USA). Anti-rabbit IgG (Cell Signaling Technology, Danvers, MA, USA) and anti-mouse IgG (Cell Signaling Technology) were used as horseradish peroxidase-conjugated secondary antibodies. The intensities of the immunoblot band were visualized and captured using an Image Quant LAS 4000 mini (GE Healthcare, Piscataway, NJ, USA). Quantification of the Western blot analysis was performed using ImageJ (National Institutes of Health, Bethesda, MD, USA).

2.4.3. Confocal microscopy

Cells on cover glass were washed with phosphate-buffered saline and fixed in 4% paraformaldehyde for 20 min. The fixed cells were permeabilized with 0.3% Triton X and stained with antibodies against fibronectin (Abcam), WT-1 (Abcam), and KLF15 (Abcam) in blocking agent overnight at 4 °C. Alexa 488/555-conjugated goat anti-rabbit antibodies (Molecular Probes, Eugene, OR, USA) were used as secondary antibodies, and 4′,6-diamidino-2-phenylindole (DAPI; Molecular Probes) was used to counterstain the nuclei. The primary antibodies were omitted in the negative controls. The sections were evaluated in a blind and random manner, and images were captured using a Leica TCS SP8 STED CW instrument (X20/0.7 numerical aperture objective lens of the DMI 6000 inverted microscope; Leica) and analyzed using MetaMorph software (version 7.8.10, Universal Imaging, Downingtown, PA, USA).

2.4.4. siRNA-mediated KLF15 knockdown in cultured podocytes

To assess the role of KLF15 in podocyte fibrosis, its expression in primary cultured podocytes was suppressed after transfection with siRNA targeting *KLF15* (sc-45567; Santa Cruz Biotechnology) according to the manufacturer's instructions. Approximately 24 h after the transfection, the cells were pressurized, using the fabricated pressuring device, for 24 h to observe the effect of *KLF15* knockdown.

2.4.5. Cell proliferation assay

Cell viability was measured using a 3-(4,5-dimethylthiazol-2-yl)-5-(3-carboxymethoxyphenyl)-2-(4-sulfophenyl)-2H-tetrazolium (MTS) cell proliferation kit (Promega) according to the manufacturer's instructions after pressurization with or without *KLF15* knockdown. The cells were incubated with the MTS reagent for 3 h at 37 °C, and the absorbance of the wells was read at 490 nm using the Epoch microplate reader (BioTek Instruments, Inc., Winooski, VT, USA).

2.4.6. Cell permeability assay

The permeability of podocytes was measured using an albumin-rhodamine transit assay. For the assay, primary cultured human podocytes were placed onto a Transwell system in 24-well plates (NUNC A/S, Roskilde, Denmark) with 0.4-μm pore membranes in DMEM/F12 (Invitrogen, Waltham, MA, USA). Albumin-rhodamine (Abcam) suspended in DMEM/F12 was added to the podocyte monolayer. The transition rate of albumin-rhodamine across the monolayer was assessed by measuring and quantifying the increase in albumin-rhodamine in the lower well 24 h later. Quantification was performed using a standard curve for albumin-rhodamine with a spectrophotometer at an excitation wavelength of 550 nm and an emission wavelength of 570 nm.

2.4.7. Detection of apoptosis

Cell apoptosis and necrosis were measured using an Annexin V/propidium iodide (PI) fluorescein isothiocyanate (FITC) apoptosis kit (BD Biosciences) via flow cytometry, according to the manufacturer's instructions, after pressurization with or without *KLF15* knockdown [17,21]. Briefly, harvested cells were washed with cold phosphate-buffered saline, resuspended in 100 μL binding buffer, stained with 5 μL FITC-conjugated Annexin V (10 mg/mL) and 10 μL PI (50 mg/mL), and incubated for 30 min at room temperature in the dark. Then, the data were acquired and analyzed with BD FACSDiva (version 8.0; BD Biosciences).

2.5. Induction of experimental chronic kidney disease (CKD) and assessment of podocyte fibrosis in mouse CKD model

2.5.1. Animal model

A mouse CKD model was developed using a modified protocol as follows [22]. Eight-week-old B6 male mice were purchased from The Jackson Laboratory (Bar Harbor, ME, USA). All experiments were performed in accordance with the Guidelines for the Care and Use of Laboratory Animals of the National Research Council and the U.S. National Institutes of Health under the approval of the Institutional Animal Care and Use Committee of the Clinical Research Institute at Seoul National University Hospital (Approval no.12–0132). Surgery was performed under anesthesia with a mixture of ketamine (100 mg/mL) and xylazine (25 mg/mL). A 1:10 dilution of the stock solution in saline was administered intraperitoneally at 0.02 mL/g body weight. Bilateral dorsal longitudinal incisions were made to expose both kidneys. The lower branch of the right renal artery was ligated with a 10.0 silk suture to produce visible renal ischemia to approximately one-third of the kidney, and the upper pole of the right kidney was amputated via electrocoagulation. Next, the upper branch of the left kidney artery was ligated, and the lower pole was placed back into the renal fossa via cauterization. Left nephrectomy was performed after 1 week (CKD day 0). The left kidney was removed, and the vascular pedicle was ligated at the hilum with 4–0 silk. The time of left nephrectomy marked the onset of moderate to severe renal failure.

2.5.2. Analysis of renal function

The animals were placed in metabolic cages to analyze renal function at 8, 16, and 20 weeks after sham surgery or 5/6 nephrectomy. Then, the animals were subjected to a 24-h urine collection regimen to determine protein and creatinine content and urine volume. Serum creatinine was also measured in blood samples from the animals. In addition, blood pressure was measured using the tail-cuff method (CODA system, Kent Scientific Corporation, Torrington, CT, USA). Mice were sacrificed at the end of the experiments, and the kidneys were harvested.

2.5.3. Histology and immunohistochemistry

Periodic acid-Schiff base (PAS) staining and Masson's trichrome staining were performed to evaluate the level of glomerular sclerosis. For the immunohistochemical assays, paraffin-embedded kidneys, cut into 4 μm-thick slices, were deparaffinized and hydrated using xylene

Table 2
Clinical characteristics of patients with hypertensive nephropathy and IgA nephropathy.

Variables	Normal kidney N = 6	IgA nephropathy N = 7	Hypertensive nephropathy N = 9	P
Age (years)	20.3 ± 2.4	25.3 ± 5.5	33.8 ± 4.9	0.001
Male sex (%)	5 (83.3)	4 (57.1)	7 (77.8)	0.519
Systolic blood pressure (mm Hg)	114.5 ± 9.2	116.6 ± 15.5	141.1 ± 14.8	0.007
Diastolic blood pressure (mm Hg)	71.5 ± 6.0	72.7 ± 10.0	88.1 ± 12.1	0.017
Estimated GFR (mL/min/1.73 m^2)	119.0 ± 11.8	106.9 ± 13.0	34.8 ± 13.9	< 0.001
Urine protein/creatinine ratio	0.2 ± 0.2	0.1 ± 0.1	0.6 ± 0.4	0.012
Urine RBC/HPF (%)				0.025
< 5	4 (66.7)	0 (0)	7 (77.8)	
5–9	0 (0)	1 (14.3)	0 (0)	
≥10	2 (33.3)	6 (85.7)	2 (22.2)	
History of hypertension (%)	0 (0)	0 (0)	9 (100)	< 0.001

Abbreviations: GFR, glomerular filtration rate; RBC, red blood cell; HPF, high power field.

and ethanol. Endogenous streptavidin activity was blocked using 3% hydrogen peroxide. The deparaffinized sections were stained with an *anti*-KLF15 antibody (Santa Cruz Biotechnology) and then incubated with horseradish peroxidase-conjugated goat anti-rabbit IgG (Vector Laboratories, Burlingame, CA, USA). Next, 3,3′-diaminobenzidine tetrahydrochloride (Sigma-Aldrich) was used for immunohistochemical detection. Finally, all sections were counterstained with Mayer's hematoxylin (Sigma-Aldrich) and evaluated under a light microscope using a camera with differential interference contrast (DFC-295; Leica).

The glomerulosclerosis index was used to quantify glomerular damage. A score for each animal was derived by examining 100 glomeruli at a magnification of × 400. The severity of scarring was expressed on an arbitrary scale from 0 to 4 as follows: 0, normal glomeruli; 1, presence of mesangial expansion or thickening of basement membrane; 2, mild/moderate segmental sclerosis involving < 50% of the tuft; 3, diffuse glomerular sclerosis involving > 50% of the tuft; and 4, diffuse glomerulosclerosis with total tuft obliteration and collapse [23].

2.6. Statistical analysis

Statistical analysis was performed using GraphPad Prism 7.0 software (Graph Pad, Inc., La Jolla, CA, USA). Data were expressed as the means ± standard deviation or means ± standard error of the mean, wherever indicated. *P*-values < 0.05 were considered statistically significant.

2.7. Ethics statement

The study protocol complies with the Declaration of Helsinki and received full approval from the institutional review board at the Seoul National University Hospital (no. H-1607-133-777). All samples were collected, stored, and monitored by the Seoul National University Hospital Human Biobank.

3. Results

3.1. KLF15 expression is decreased in renal tissue from patients with hypertensive nephropathy

We first analyzed the level of KLF15 expression in renal biopsies obtained from patients with biopsy-proven hypertensive nephropathy (n = 9) compared to that of IgA nephropathy (n = 7) and normal kidney (n = 6) controls. The systolic and diastolic blood pressures of hypertensive nephropathy patients were significantly higher than those of IgA nephropathy patients and normal kidney controls, and renal function was also significantly lower than that in both controls. Detailed information on hypertensive nephropathy and control patients can be found in Table 2. Upon quantifying the expression of KLF15 by immunofluorescence, KLF15 expression was significantly lower in hypertensive nephropathy patients than in both healthy and disease controls (Fig. 1). Based on the findings in human renal tissue, an *in vitro* study, simulating hypertensive injury with the mechanical device, was conducted to investigate the effects of KLF15 on various levels of hypertensive renal injury.

3.2. Successful isolation of primary cultured podocytes derived from human kidney tissue

First, the podocytes were cultured and isolated to obtain cells for *in vitro* experiments. Similar to our previous study [19,24], we harvested 200–300 glomeruli from kidney tissue, and the isolated glomeruli were cultured for 8 days. Cells growing from the isolated glomeruli consisted of three major glomerular resident cells (podocytes, mesangial cells, and endothelial cells) and showed cobblestone-like morphology. As the origin of the cells was heterogeneous, we purified podocyte-derived cells from other glomerular-resident cells using FACS. The glomerular cells were stained with CD90 and podocalyxin to distinguish between mesangial cells and podocytes before sorting using FACS. Cells that were CD90-negative and podocalyxin-positive were considered a homogeneous collection of podocyte-derived cells. Flow cytometric analysis revealed that 32.8 ± 10.6% cells were podocytes, and thus 3.2×10^5 podocytes were collected from 1×10^6 cells for further analysis (Supplementary Figure 1A). The purity of the collected podocytes was verified based on the immunofluorescence expression of synaptopodin, nephrin, and CD31 using confocal microscopy. No CD31 expression was detected, and only synaptopodin and nephrin expression were observed in the podocytes. The purity of the collected podocytes was > 98% (Supplementary Figure 1B). The mesangial and endothelial cells were also sorted identically using CD90 and CD31, respectively.

3.3. Cell viability is significantly reduced with pressure applied by rotational force

Unlike conventional chemically induced hypertensive injury models, we designed a novel device to create a more physiologic hypertensive model through mechanical injury. To implement mechanical damage *in vitro*, the device, based on the design of the centrifuge, was constructed to apply sustained pressure to the cultured cells (Fig. 2). Detailed information on specific device components and features can be found in the Materials and Methods section. With this device, we were able to apply vertical pressure to the cells using rotational force applied to the cell culture dish placed on the mounting dock.

To confirm that the proposed device generates rotational force-driven pressure inside the culture dish, we measured pressure using a digital pressure sensor in five experiments (Fig. 3A). As the number of rotations per minute was sequentially increased from 100 to 350, the pressure levels changed from 0.4 to 13.4 mmHg (Table 3). The device

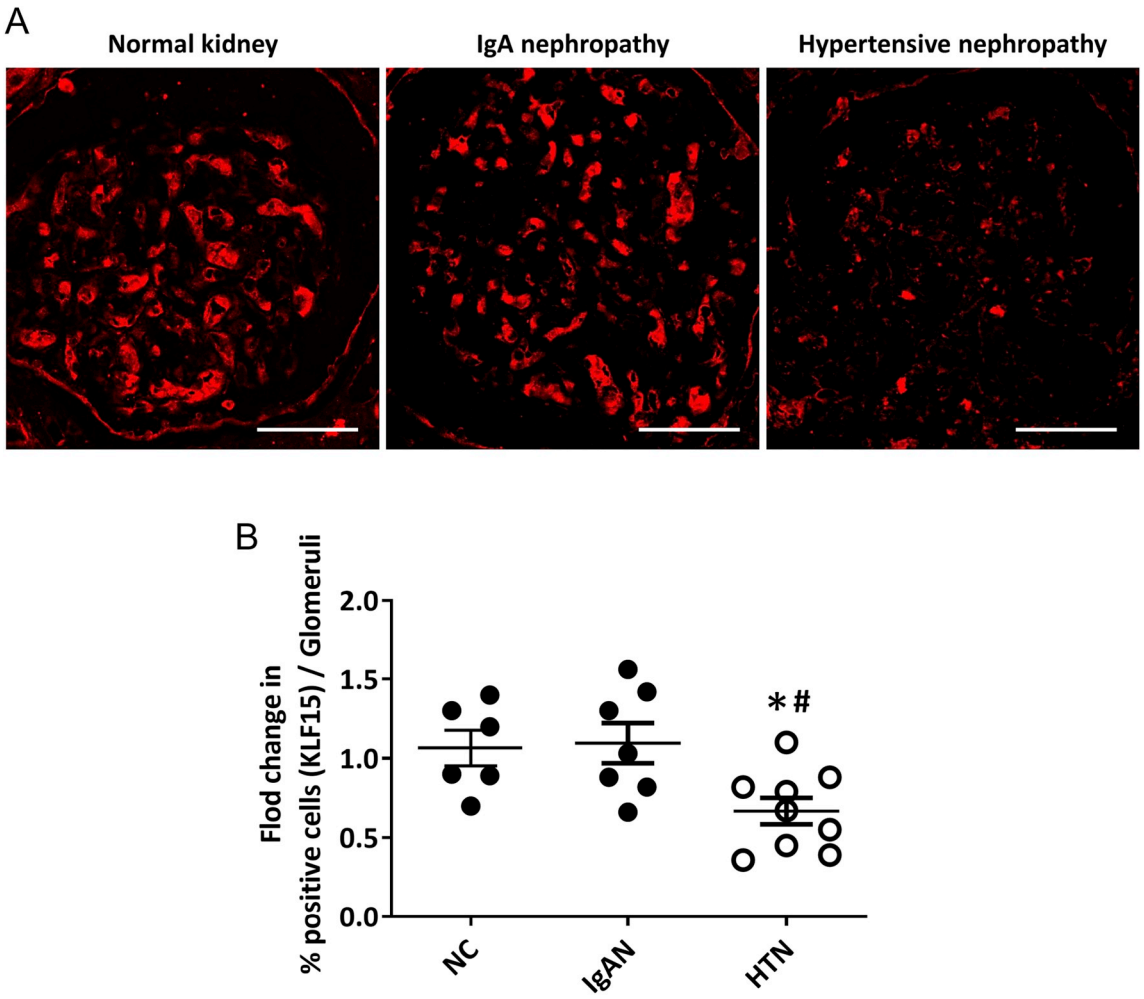

Fig. 1. KLF15 expression is decreased in human kidneys with biopsy-proven hypertensive nephropathy compared to that in human kidneys with IgA nephropathy or normal kidneys. A, Representative immunofluorescence images from glomeruli of patients with hypertensive nephropathy, IgA nephropathy, and normal kidneys. Original magnification, × 600. Scale bars: 50 μm. B, Difference in glomerulus area showing KLF15 expression in normal kidneys and those with IgA nephropathy and hypertensive nephropathy (*, $P < 0.05$ compared with normal kidney; #, $P < 0.05$ compared with kidney with IgA nephropathy). NC, normal kidney control; IgAN, IgA nephropathy control; HTN, hypertensive nephropathy.

was suitable for operation in an incubator because it was stable without shaking and generated low amounts of heat, and thus did not affect the temperature in the incubator. To determine the pressure level required to induce podocyte injury, the podocytes were cultured under 0–10 mmHg, and cell viability was analyzed by counting the number of live cells after applying each pressure condition for 48 h. The viability of podocytes cultured at pressures below 4 mmHg did not differ significantly from those cultured under static conditions. However, the cell survival rate decreased significantly for podocytes cultured at pressure levels over 8 mmHg, and most podocytes were not viable at pressures above 10 mmHg (Fig. 3B). In addition, we observed a reduction in the viability of mesangial and glomerular endothelial cells upon pressurization, which was similar to that observed for podocytes (Supplementary Figure 2). That is, we succeeded in applying various levels of pressure to different types of renal cells using a novel device, and we identified decreases in cell viability as the pressure applied by rotational force increased.

3.4. Podocyte differentiation decreases and fibrosis increases with mechanical pressurization by rotational force

Based on the aforementioned results, we applied 4 and 8 mmHg pressure to evaluate fibrosis and conduct subsequent experiments. To determine whether pressure alters the differentiation of primary cultured podocytes, confocal microscopy was performed to determine the expression patterns of WT-1, a podocyte differentiation marker, and KLF15, a transcription factor that mediates cell differentiation (Fig. 4A). As the applied pressure was increased to 0, 4, and 8 mmHg, WT-1 and KLF15 expression decreased proportionally. Fibronectin expression was also analyzed using confocal microscopy to assess fibrosis induction in podocytes. As expected, fibronectin expression increased with elevations in pressure using the proposed device (Fig. 4B). Quantification of mRNA expression levels using PCR revealed that application of 4 mmHg pressure to podocytes for 48 h significantly increased fibronectin expression and reduced the expression of multiple podocyte differentiation markers including WT-1, podocalyxin, and synaptopodin. KLF15 expression after culture under 4 mmHg pressure was lower than that under static conditions (Fig. 4C). Western blot analysis showed results similar to that of mRNA expression analysis. In addition, the expression of ZO-1, a junction marker in podocytes, was lower under pressure conditions than under static conditions (Fig. 4D). Thus, we verified that KLF15 expression is associated with fibrosis and altered podocyte differentiation through various experimental methods.

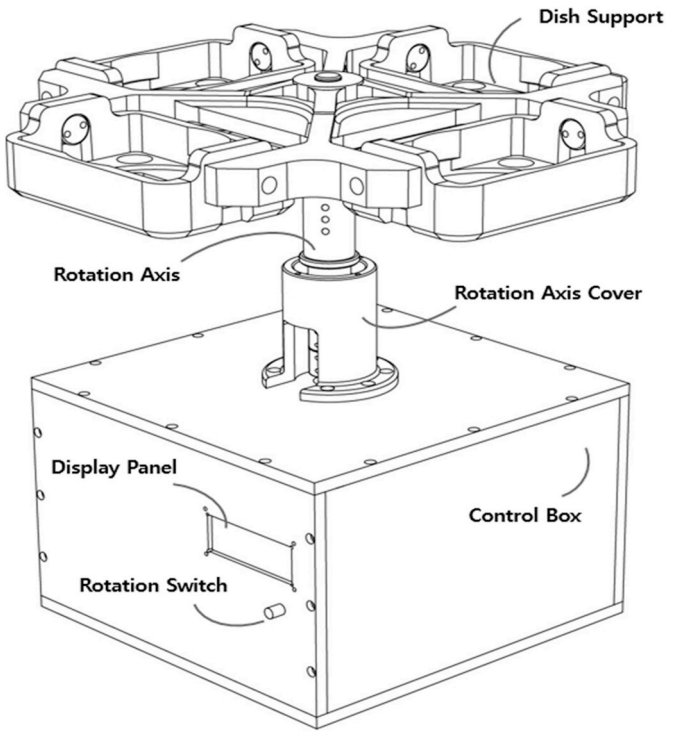

Fig. 2. Schematic diagram of a mechanical stress device used to generate pressure via rotational force. Cell culture dishes used in typical cell culture experiments can be mounted on the dish support. The mounting part rotates around the rotation axis at a constant speed set by the researcher. During circular motion, the dish rotates outward with the pivot located on both sides of the mounting part as the central axis according to the direction of the rotational force transmitted to the dish. The display panel of the control box displays the rotational speed as RPM and the corresponding pressure for RPM.

3.5. RA effectively increases KLF 15 expression under rotational force pressure and under static conditions

RA, a well-known activator of KLF15, was administered under each condition to compare podocyte differentiation according to changes in KLF15 expression under normotensive and mechanically induced hypertensive conditions (Fig. 5A). Under hypertensive conditions, the mRNA levels of *KLF15* and synaptopodin were significantly reduced, which was indicative of podocyte dedifferentiation after hypertensive injury. The levels of synaptopodin and KLF15 increased significantly after RA administration in both normotensive and hypertensive conditions, suggesting that KLF15 is an important regulator of podocyte differentiation during hypertensive injury.

3.6. KLF15 knockdown increases fibrosis, cell to cell junctional impairment, and cytotoxicity after pressurization

Compared to that with the scrambled control siRNA, siKLF15 significantly suppressed *KLF15* expression (Fig. 5B). After the application of 4 mmHg pressure for 24 h, the expression of fibronectin and α-smooth muscle actin (α-SMA) was further increased in siKLF15-transfected cells compared to that in pressurized control cells, whereas ZO-1 expression was significantly reduced (Fig. 5C). Because of the dramatic change in ZO-1 protein expression, we conducted albumin-rhodamine transit assay to assess the role of KLF15 in the permeability of podocytes to albumin. After 24 h, the absorbance of human serum albumin-rhodamine in the medium of the lower chamber was higher after pressurization compared to that under static conditions. Moreover, *KLF15* knockdown further increased the permeability of pressurized cells (Fig. 5D). Since functional alterations to podocytes might have resulted

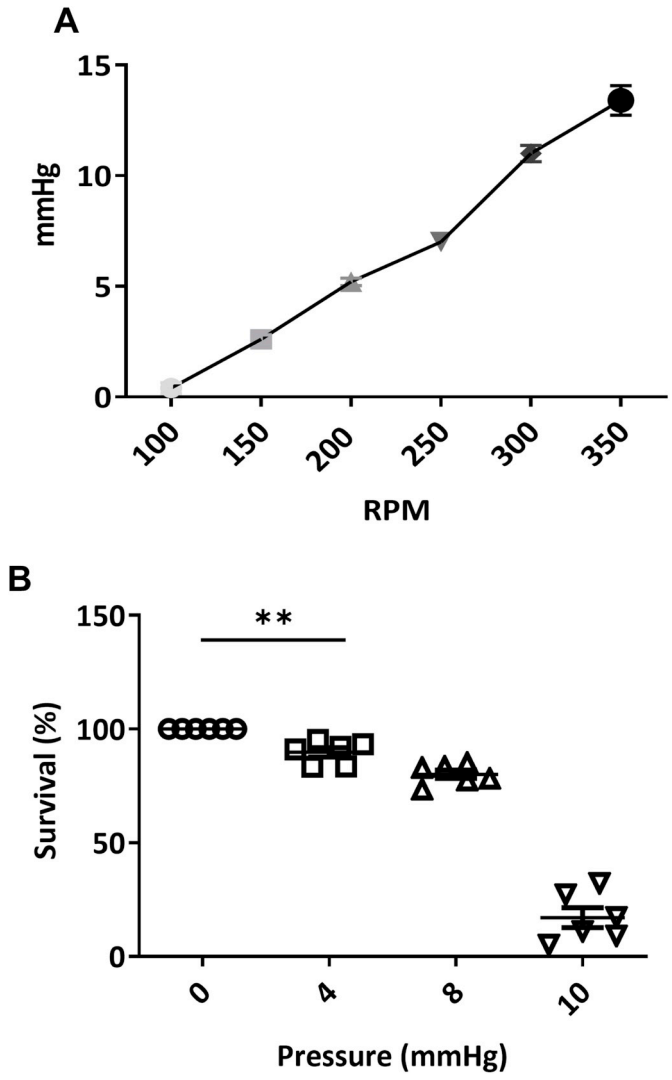

Fig. 3. Optimization of pressure applied to cells to construct a disease model of hypertensive injury *in vitro* using a novel rotational force-based pressurizing device. A, Pressure increased with revolutions per minute. The average pressure was calculated from five replicates to obtain a standard speed–pressure curve. B, Cell survival rates decreased significantly with increases in pressure levels over 48 h (**, $P < 0.01$). RPM, rotations per minute; AVR, average.

from cell death, we assessed cell viability and apoptosis. For MTS assays, compared to both control cells under non-pressurized and pressurized conditions, pressurized cells with *KLF15* knockdown exhibited a statistically significant increase in cytotoxicity (Fig. 5E). Furthermore, apoptotic cells were increased after pressurization, and KLF15 knockdown exacerbated this. In the pressurized state, the number of apoptotic cells was significantly reduced after RA treatment. However, the effect of RA was reduced after KLF15 knockdown (Fig. 5F). Collectively,

Table 3
Pressure (in mmHg) measured with rotations per minute.

RPM	100	150	200	250	300	350
1st	1	3	5	7	10	11
2nd	1	3	6	7	10	12
3rd	0	2	5	7	11	15
4th	0	2	5	7	12	14
5th	0	3	5	7	12	15
Average	0.4	2.6	5.2	7	11	13.4

Abbreviation: RPM, rotations per minute.

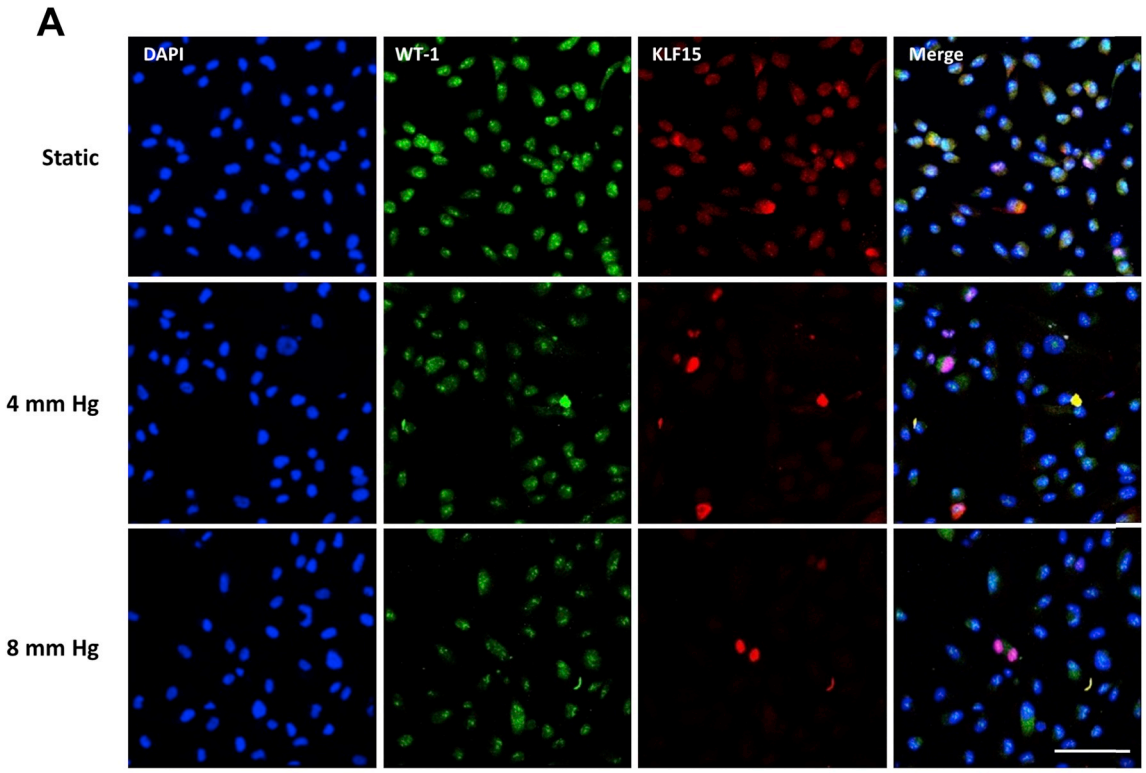

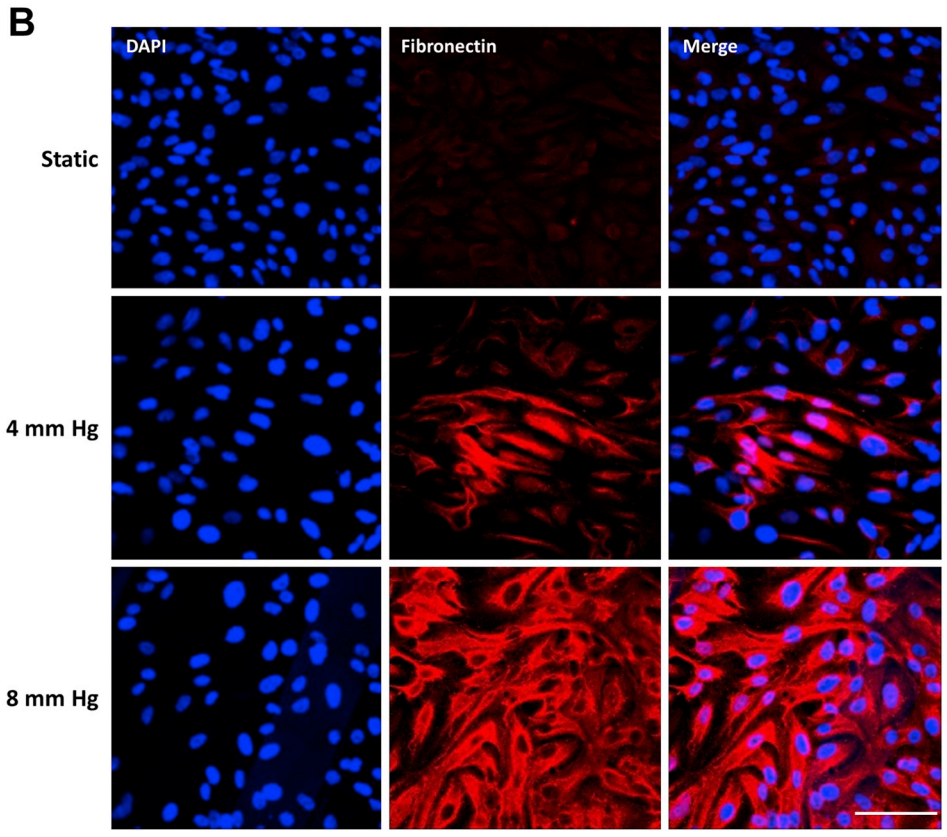

(caption on next page)

Fig. 4. Effect of pressure induced by rotational force on primary cultured podocytes. A, Detection of WT-1 and KLF15 expression by immunofluorescence staining. DAPI (nucleus, blue), WT-1 (green), and KLF15 (red). Original magnification, × 400. Scale bars: 50 μm. B, Detection of fibronectin expression by immunofluorescence staining. DAPI (nucleus, blue), fibronectin (red). Original magnification, × 400. Scale bars: 50 μm. C, Fibronectin, *WT-1*, *KLF15*, podocalyxin, and synaptopodin mRNA levels were measured under static and pressure conditions after applying 4 mmHg for 48 h. D, Western blot analysis was performed for fibronectin, WT-1, KLF15, and ZO-1. The representative blot of three independent experiments is shown. The densitometric analysis of these blots is shown on the right side (n = 3, ***, $P < 0.001$).

the knockdown of KLF15 exacerbates fibrosis, podocyte dysfunction, and cytotoxicity in pressurized cells.

3.7. Mechanically induced hypertension induces fibrosis, and this injury is restored by RAS inhibition, as in a chemically induced hypertension model

To compare the mechanically induced hypertension model developed in our study with the existing chemically induced RAS-activated hypertension model, we assessed the expression of fibrosis markers and KLF15 after hypertensive injury using angiotensin II (Fig. 6). After the administration of 10^{-6} M angiotensin for 48 h, we observed a significant decrease in KLF15 and an increase in α-SMA expression; there was no difference in the expression of either protein when compared to levels observed under physically induced hypertensive conditions. In addition, losartan, an angiotensin type 1 receptor blocker, was administered to determine if fibrosis and KLF15 levels could be restored after RAS inhibition in a mechanically induced hypertension model. We observed a decrease in α-SMA and an increase in KLF15 expression after losartan treatment in a dose-dependent manner. Therefore, we confirmed that the antifibrotic effect of KLF15 on mechanically induced hypertension in the present study was similar to that with the conventional chemically induced hypertension model.

3.8. KLF 15 expression is reduced in a chronic hypertensive renal injury murine model induced by 5/6 nephrectomy

We next used 5/6 nephrectomized CKD mice to determine the role of KLF15 in hypertension and fibrosis *in vivo*. Kidney injury markers such as the urine protein/creatinine ratio and serum creatinine increased sequentially with time after 20 weeks of nephrectomy (Fig. 7A). The systolic blood pressure measured every 8 weeks showed continuous elevation, and the final blood pressure measured was 150.5 ± 8.9 mmHg at 20 weeks. We also evaluated changes in body weight gain as another surrogate marker of injury. Nephrectomy

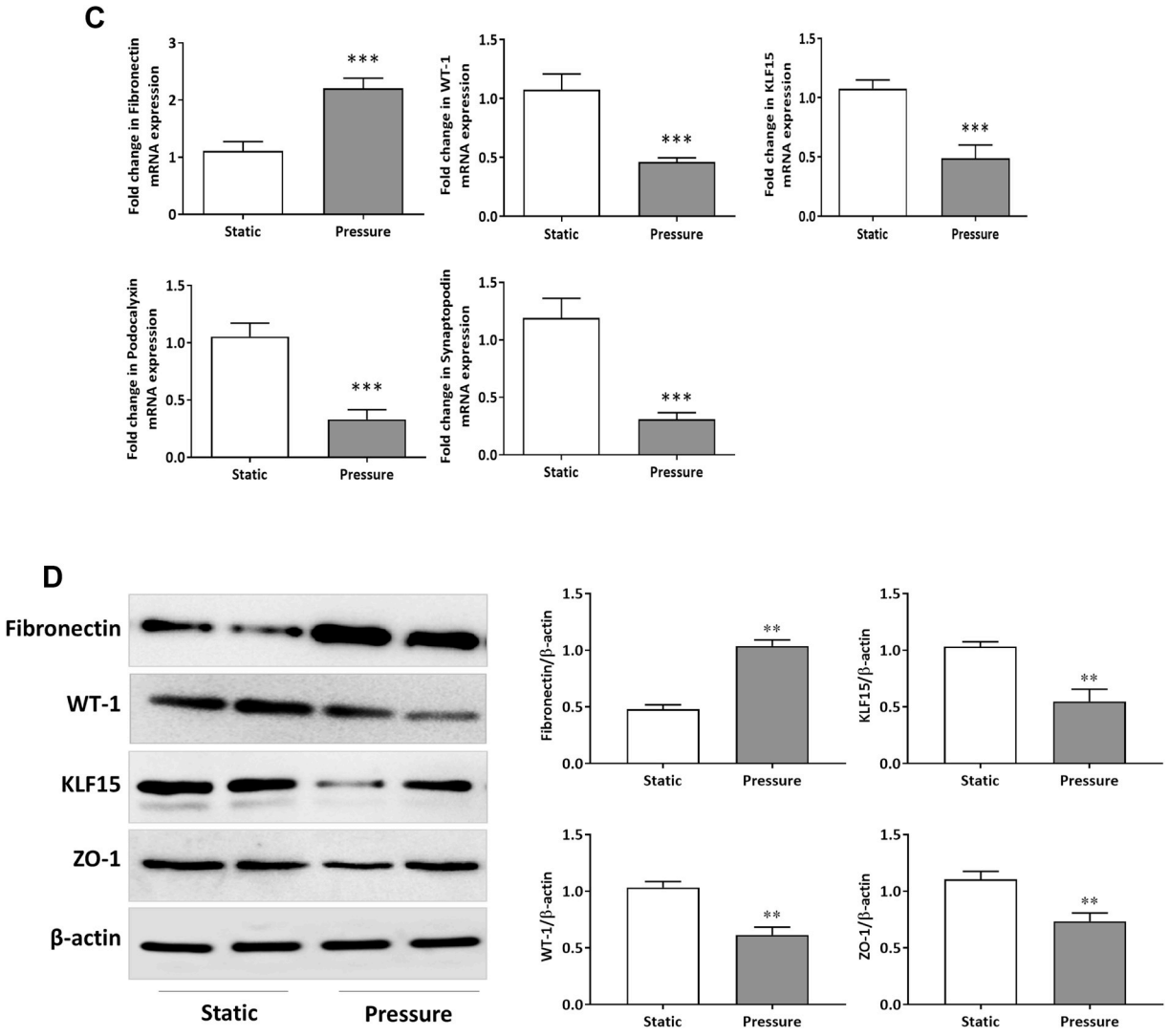

Fig. 4. (*continued*)

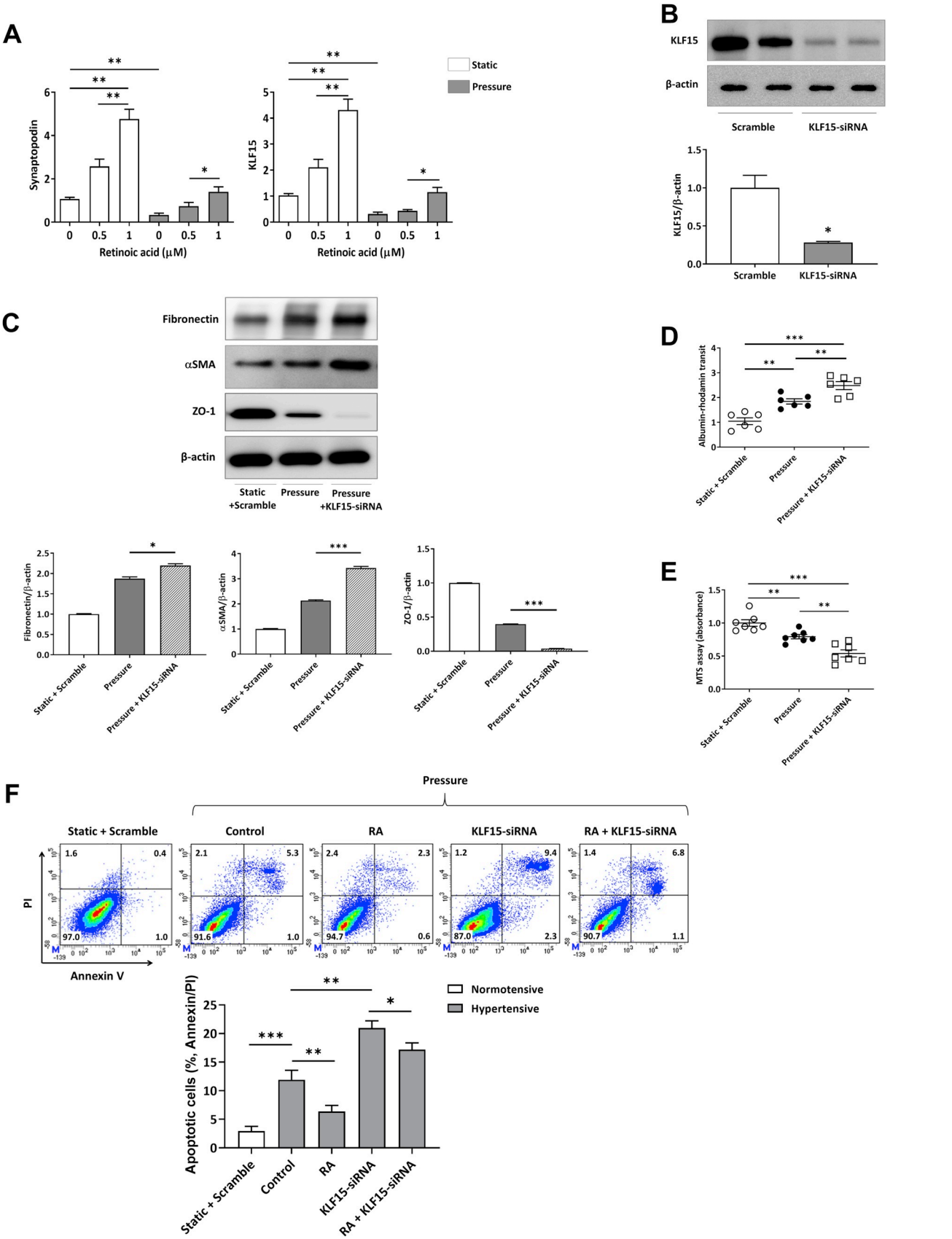

(caption on next page)

Fig. 5. Effect of KLF15 on pressure-induced injury in human podocytes after activation and knockdown of *KLF15*. A, The dose-dependent changes in *synaptodin* (left) and *KLF15* (right) mRNA expression levels were assessed by administering various doses of retinoic acid (RA) to activate KLF15 expression. The increase in RA-induced *KLF15* expression was significant not only under static conditions (white bars), but also under the pressurized condition with 4 mmHg for 48 h (gray bars). This was accompanied by an increase in *synaptodin*, a marker of differentiated podocytes. B, A representative Western blot shows that KLF15 expression was appropriately inhibited after siRNA transfection. The densitometric analysis of these blots is shown in the lower panel (*, $P < 0.05$). C, The increase in fibrosis and loss of tight junctions after KLF15 inhibition in rotational force-induced hypertensive conditions were measured. Expression of fibrosis markers fibronectin and α-SMA, as well as ZO-1, a tight junction-related protein, as determined by western blotting. The representative plots are shown in the upper left. Blots showing the expression of these proteins were quantified and expressed as densities (n = 3, *, $P < 0.05$, ***, $P < 0.001$). D, Relative quantification of albumin-rhodamine transit across monolayers of podocytes treated with vehicle (**, $P < 0.01$; ***, $P < 0.001$). E, Cell cytotoxicity assay after pressurization with or without *KLF15* knockdown. *KLF15* knockdown aggravated the decrease in cell viability, as measured using the MTS assay under hypertensive condition (**, $P < 0.01$; ***, $P < 0.001$). E, Annexin V/propidium iodide (PI) staining assay. Apoptotic cells were decreased with RA treatment in the pressurized condition compared to those under pressure alone; however, after KLF15 knockdown, the reduction in apoptotic cells mediated by RA was alleviated (*, $P < 0.05$; **, $P < 0.01$; ***, $P < 0.001$). All experiments with siRNA transfection were performed under pressurized conditions (4 mmHg for 24 h).

resulted in significantly less weight gain with a final weight of 23.5 ± 0.9 g in the 5/6 nephrectomized group, compared to 29.7 ± 1.0 g in the sham-operated group (Fig. 7B). Histopathological findings at 20 weeks after 5/6 nephrectomy showed that glomerular fibrosis increased with time, and global sclerosis with diffuse deposits of fibrotic material in the glomerulus was observed after PAS and Masson's trichrome staining. Furthermore, immunohistochemical staining showed that KLF15 expression decreased with fibrosis progression (Fig. 7C). The indices of glomerulosclerosis also increased, and the percent of glomeruli containing KLF15-positive cells decreased with time (Fig. 7D). Compared to that observed in sham-operated mice, fibronectin expression increased significantly and KLF15 expression decreased in 5/6 nephrectomized mice (Fig. 7E). The levels of CCN1 and β-galactosidase, which are cell senescence markers, as well as that of fibronectin, increased with the progression of chronic injury, and the mRNA levels of *KLF15* decreased with time, compared to those of other fibrosis and senescence markers (Fig. 7F). Thus, in animal CKD models, we found that KLF15 expression is closely associated with fibrosis similar to that observed in *in vitro* experiments.

4. Discussion

In this study, we established a mechanically induced hypertensive cell injury model using rotational force. In this mechanical injury model, fibrosis progression and concomitant changes in KLF15 expression were observed. Furthermore, the antifibrotic effects of KLF15 were confirmed by experiments with KLF15 activation and knockdown. These changes in KLF15 expression were also observed in an *in vivo* model of hypertensive injury using 5/6 nephrectomized mice. Therefore, KLF15 plays an important role in fibrosis associated with hypertensive injury.

Previous studies have attempted to mimic hypertensive injuries in kidney cells *in vitro* [25,26], although studies on the direct application of mechanical pressure to cells are lacking. Although chemically induced fibrosis, such as that induced upon treatment with angiotensin II or TGF-β, is commonly used to prepare experimental models of hypertensive glomerulopathy [14–17], these fibrosis models do not recapitulate the entire mechanism of cell damage associated with hydrostatic pressure. Previously, a research group attempted to apply pressure to cells using a pressurizable incubation chamber and evaluate

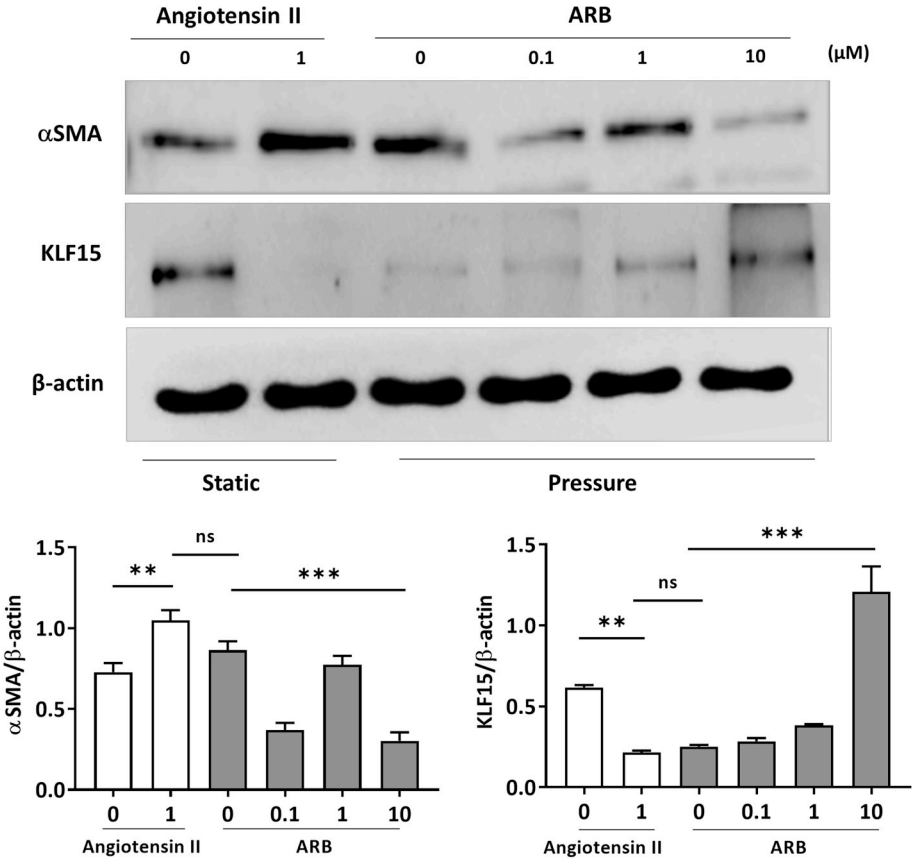

Fig. 6. Comparison of chemically or mechanically induced hypertension models and response to antihypertensive treatment in the rotational force-induced model of mechanical hypertension. To compare the mechanically induced hypertension model developed in this study with the previously developed renin-angiotensin system (RAS)-activated chemically induced hypertension model, the expression of fibrosis markers and KLF15 after angiotensin II-induced hypertensive injury was assessed. Furthermore, an angiotensin type 1 receptor blocker (ARB) was administered at varying doses to determine whether this standard hypertension treatment relieved the damage caused by the mechanically induced hypertensive model. A representative Western blot (upper) and quantification of the blots (lower) are shown (ns, not significant; **, $P < 0.01$; ***, $P < 0.001$).

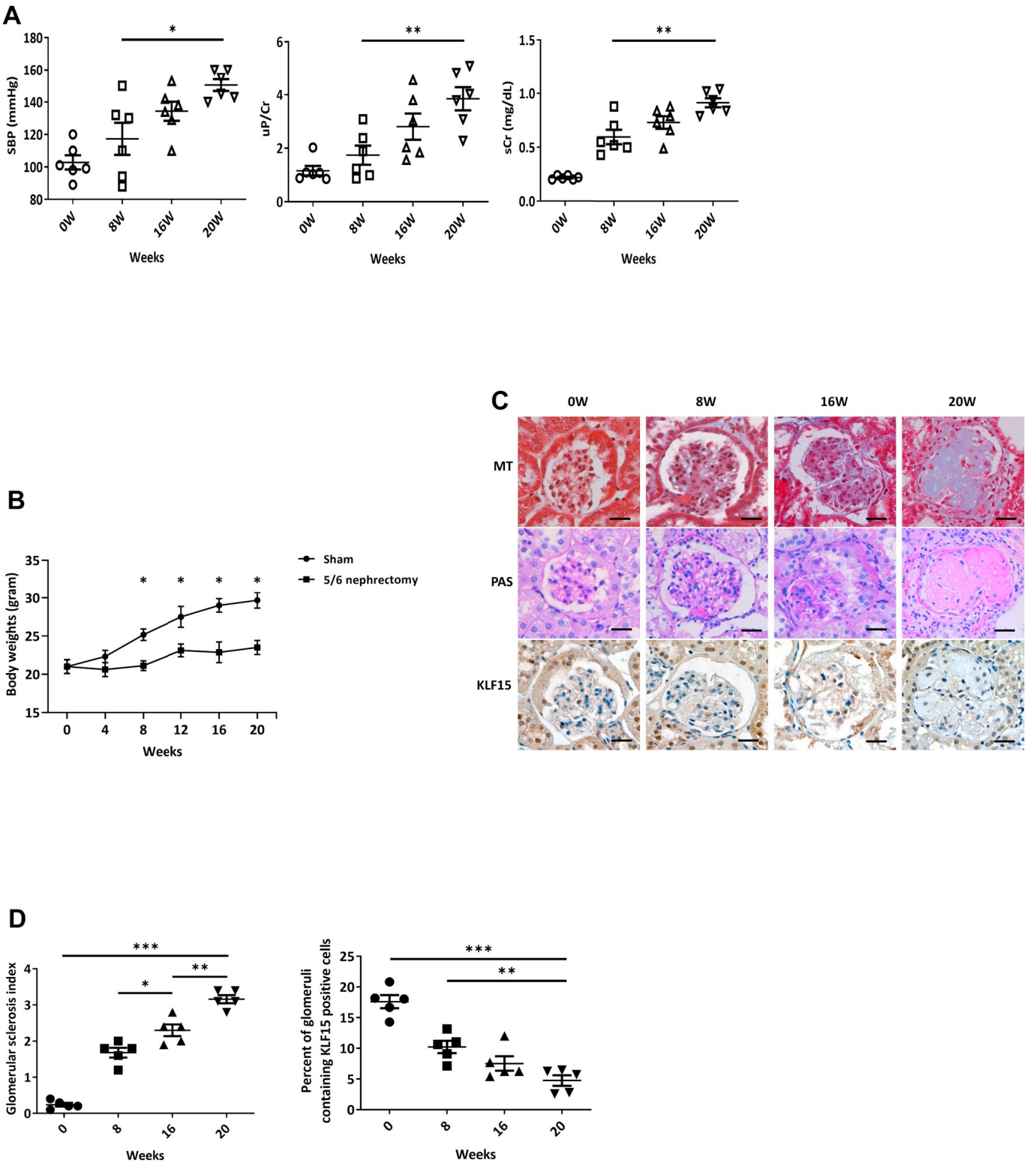

Fig. 7. Changes in KLF15 expression-associated elevated blood pressure and the progression of fibrosis in chronic kidney disease (CKD) animal models. A, Systolic blood pressure and proteinuria gradually increased during 20 weeks after 5/6 nephrectomy in wild-type mice, whereas renal function gradually decreased (*, $P < 0.05$; **, $P < 0.01$). B, Mice were weighed after every 8 weeks during the experimental protocol. C, Representative PAS and MT staining images at 0, 8, 16, and 20 weeks showed progressive increases in glomerular fibrosis. Immunohistochemical staining showed that KLF15 expression decreased in the glomerulus over time. Original magnification, × 400. Scale bars: 50 μm. D, In CKD mice, the mean glomerulosclerosis index was 3.2 ± 0.3 at 20 weeks of disease. The percentage of glomeruli containing KLF15-positive cells was significantly reduced after developing CKD, from 17.6% to 4.8% (*, $P < 0.05$; **, $P < 0.01$; ***, $P < 0.001$). E, A representative Western blot showing fibronectin and KLF15 expression in a sham-operated mouse and 5/6 nephrectomized mouse at 20 weeks. Quantification of the blot showed a significant increase in fibronectin and a decrease in KLF15 expression after 5/6 nephrectomy (**, $P < 0.01$; ***, $P < 0.001$). F, Levels of senescence markers (CCN1 and β-galactosidase), fibronectin, and KLF15 were quantified and shown as densitometry plots (*, $P < 0.05$; ***, $P < 0.001$). SBP, systolic blood pressure; uP/Cr, urine protein to creatinine ratio; sCr, serum creatinine; MT, Masson's trichrome; PAS, Periodic acid-Schiff base; Sham, sham-operated mice; 5/6 CRF, 5/6 nephrectomized mice.

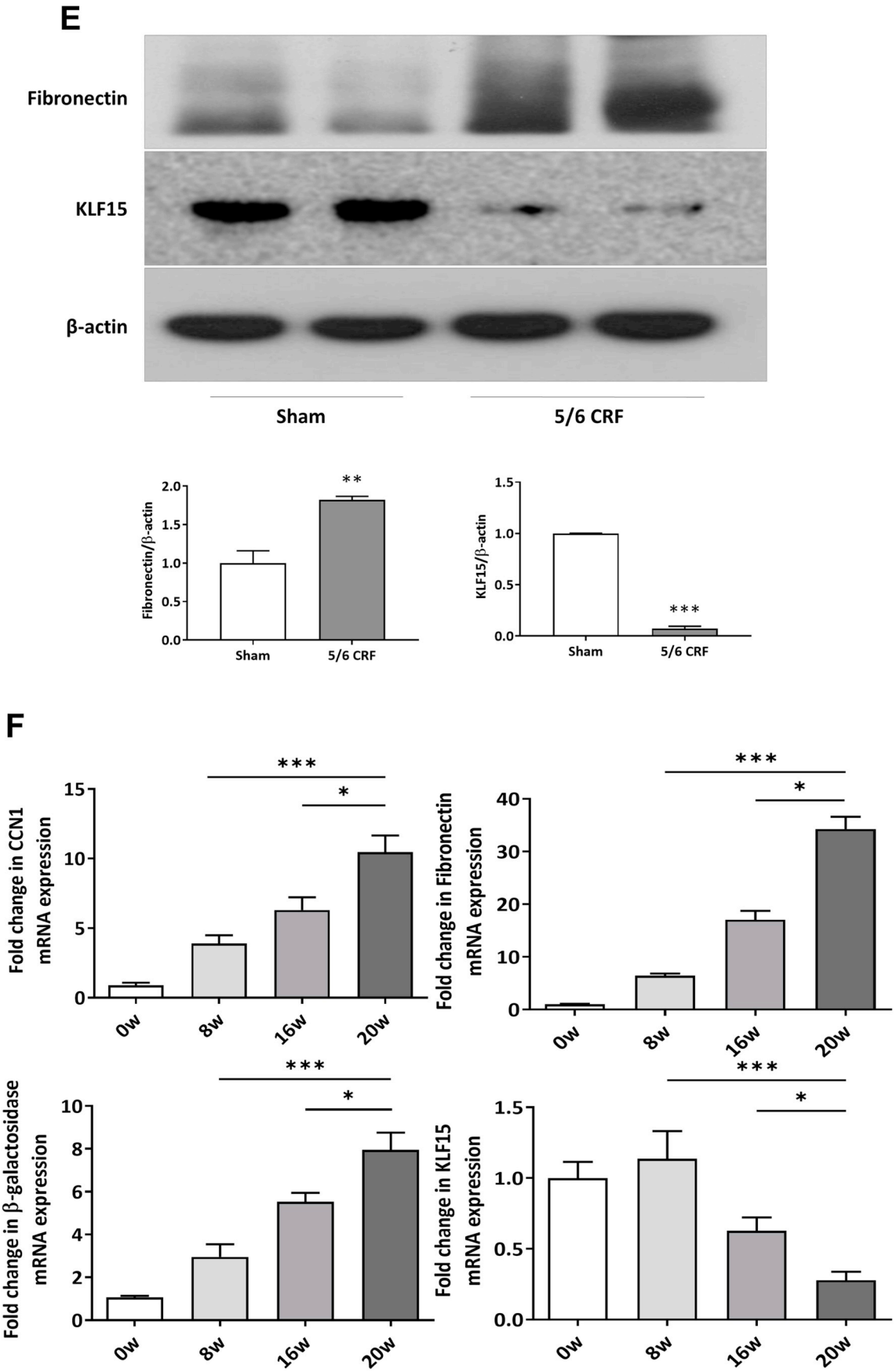

Fig. 7. (*continued*)

the effect of pressure on dermal fibroblasts during senescence [27]. In that study, the applied pressures of 60 and 120 mmHg were higher than atmospheric pressure [27]. Pressure can be applied uniformly to cells in all directions in a pressurizable incubation chamber; however, the application of unidirectional pressure to achieve filtration pressure on the cells surrounding the glomerular capillary in kidneys is more physiologically relevant. In our study, the glomerular filtration pressure was simulated effectively *in vitro* by applying unidirectional pressure to the cells using a simple rotational device. Our analysis showed that fibrosis was effectively induced in podocytes by only 4–8 mmHg of unidirectional pressure.

KLF15 belongs to a 17-member family of DNA-binding zinc finger transcription factors known to be involved in a broad range of cellular processes including differentiation, mitochondrial biogenesis, cell cycle, and DNA repair [6,28,29]. We previously showed that KLF15 is closely related to the RA-induced differentiation of primary cultured podocytes [19], which was confirmed in this study. Although the effect of RA on the expression of podocyte differentiation-associated mRNA was not as significant under normal conditions as under pressure conditions, we observed that the levels of KLF15 and synaptopodin, which were significantly reduced by pressure, increased dose-dependently with RA. Previously, RA has been shown to increase the binding of KLF15 to the promoter regions of genes encoding nephrin and podocin, and KLF15 mRNA and protein levels are known to be elevated in differentiated podocytes [6]. Our results are consistent with those of previous studies in terms of the effect of KLF15 on RA-induced podocyte differentiation, as well as the protective effect of RA on podocyte injury after hypertensive damage. In addition, our study also demonstrated the association between fibrosis and KLF15 under pressure using siRNA-mediated knockdown of *KLF15*. A recent study by Gu et al. showed that KLF15 acts as an early anti-fibrotic transcriptional regulator in angiotensin II-induced renal fibrosis [3], which is in agreement with the results of this study. Furthermore, studies on the 5/6 nephrectomy model showed a significant progression of glomerular sclerosis with elevations in blood pressure. The reduction in KLF15 expression, along with the increase in the expression of fibrosis markers, indicated that KLF15 is associated with fibrosis progression, as well as podocyte dedifferentiation. The reduced expression of KLF15 in tissues of patients with hypertensive renal impairment also supports these results.

In our study, a newly developed mechanical device was used to induce fibrosis injury to a degree similar to that induced by angiotensin II-induced chemical hypertensive injury. Compared to the angiotensin II-based conventional hypertension model, our model can affect not only the renin-angiotensin pathway but also various other molecules and growth factors that might be involved in “real” hypertension. Thus, we have established a novel *in vitro* experimental method to mimic actual *in vivo* hypertensive renal damage. As previous studies have shown differences in gene and protein expression between the angiotensin II-induced hypertension model and the mechanistic stretch-induced tension in cardiac myocytes, hypertensive injury in the kidney might also proceed via mechanisms other than the angiotensin II-associated pathway [30]. Therefore, in addition to studies using chemically induced hypertension, our novel device is expected to be useful for various other mechanistic studies related to hypertensive kidney disease. In addition, it can be used as a tool to bridge the gap between *in vivo* and clinical research by creating physiological environments that mimic those found in hypertensive diseases using appropriate pressure.

Our study has demonstrated the association between hypertensive nephropathy and the transcription factor KLF15, which was the strength of the study. However, our study also has several limitations. First, the device used in our study applies pressure to cells in the vertical direction, similar to the action of filtration pressure; however, the shear stress of the glomerular capillary and urinary space were not evaluated. Shear stress cannot be eliminated in our device; hence, we are now developing a device that combines the flow rate with the current pressurizing device. Second, whether the pressure applied in this study is similar to that applied to podocytes in the human glomerulus cannot be determined. Although the glomerular capillary pressure in rodent kidneys is approximately 45–55 mmHg [31,32], data from the direct measurement of glomerular capillary pressure in humans are lacking. Furthermore, the actual pressure applied to each cell in the human body is difficult to calculate. Studies on KLF15-related transcriptomes and in-depth pathway analyses of hypertensive injury and fibrosis are required, which might lead to the development of a therapeutic approach to modulate KLF15. In summary, our study demonstrated the role of KLF15, a transcription factor associated with renal fibrosis and podocyte differentiation, using a model of hypertensive renal injury, which causes physical damage to cells via rotational force device.

Author Contribution

Mi-Yeon Yu and Ji Eun Kim designed the experiment, analyzed the data, wrote the manuscript and equally contributed to this manuscript. Saram Lee and Jin Woo Choi performed the experiments and solved technical problems. Yong Chul Kim, Seung Seok Han, Hajeong Lee, Ran Hui Cha, Jung Pyo Lee, Jae Wook Lee, Dong Ki Kim and Yon Su Kim formed the hypothesis and discussed results. Seung Hee Yang directed and coordinated the project, developed the in vivo assays and designed the experiments.

Declaration of competing interest

None.

Acknowledgments

We thank Prof. Hee Chan Kim (Seoul National University, Seoul) for his valuable technical support regarding this study. This research was supported by Basic Science Research Program through the National Research Foundation of Korea (NRF) funded by the Ministry of Science, ICT & Future Planning (grant number: 2018R1D1A1B07050196).

Appendix A. Supplementary data

Supplementary data to this article can be found online at https://doi.org/10.1016/j.yexcr.2019.111706.

References

[1] B.B. McConnell, V.W. Yang, Mammalian Kruppel-like factors in health and diseases, Physiol. Rev. 90 (4) (2010) 1337–1381.
[2] M.J. Rane, Y. Zhao, L. Cai, Krupsilonppel-like factors (KLFs) in renal physiology and disease, EBioMedicine 40 (2019) 743–750.
[3] X. Gu, D. Xu, L. Fu, Y. Wang, C. Mei, X. Gao, KLF 15 works as an early anti-fibrotic transcriptional regulator in Ang II-induced renal fibrosis via down-regulation of CTGF expression, Kidney Blood Press. Res. 42 (6) (2017) 999–1012.
[4] X. Gao, G. Wu, X. Gu, L. Fu, C. Mei, Kruppel-like factor 15 modulates renal interstitial fibrosis by ERK/MAPK and JNK/MAPK pathways regulation, Kidney Blood Press. Res. 37 (6) (2013) 631–640.
[5] X. Gu, S.K. Mallipattu, Y. Guo, M.P. Revelo, J. Pace, T. Miller, et al., The loss of Kruppel-like factor 15 in Foxd1(+) stromal cells exacerbates kidney fibrosis, Kidney Int. 92 (5) (2017) 1178–1193.
[6] S.K. Mallipattu, R. Liu, F. Zheng, G. Narla, A. Ma'ayan, S. Dikman, et al., Kruppel-like factor 15 (KLF15) is a key regulator of podocyte differentiation, J. Biol. Chem. 287 (23) (2012) 19122–19135.
[7] P.A. Sarafidis, P.I. Georgianos, P.E. Zebekakis, Comparative epidemiology of resistant hypertension in chronic kidney disease and the general hypertensive population, Semin. Nephrol. 34 (5) (2014) 483–491.
[8] S. Udani, I. Lazich, G.L. Bakris, Epidemiology of hypertensive kidney disease, Nat. Rev. Nephrol. 7 (1) (2011) 11–21.
[9] S. Kim, Y.R. Song, H.J. Chin, Y.K. Oh, K.H. Oh, K.W. Joo, et al., The prevalence of chronic kidney disease and the predictors of decreased kidney function in hypertensive patients, Kidney Res Clin Pract 27 (1) (2008) 20–27.
[10] A. Petermann, J. Floege, Podocyte damage resulting in podocyturia: a potential diagnostic marker to assess glomerular disease activity, Nephron Clin. Pract. 106 (2) (2007) c61–c66.
[11] V.G. Puelles, L.A. Cullen-McEwen, G.E. Taylor, J. Li, M.D. Hughson, P.G. Kerr, et al.,

Human podocyte depletion in association with older age and hypertension, Am. J. Physiol. Renal. Physiol. 310 (7) (2016) F656–F668.
[12] G.S. Hill, D. Heudes, J. Bariety, Morphometric study of arterioles and glomeruli in the aging kidney suggests focal loss of autoregulation, Kidney Int. 63 (3) (2003) 1027–1036.
[13] G.S. Hill, Hypertensive nephrosclerosis, Curr. Opin. Nephrol. Hypertens. 17 (3) (2008) 266–270.
[14] Z. Xu, W. Li, J. Han, C. Zou, W. Huang, W. Yu, et al., Angiotensin II induces kidney inflammatory injury and fibrosis through binding to myeloid differentiation protein-2 (MD2), Sci. Rep. 7 (2017) 44911.
[15] Y. Shen, N. Miao, J. Xu, X. Gan, D. Xu, L. Zhou, et al., Metformin prevents renal fibrosis in mice with unilateral ureteral obstruction and inhibits Ang II-induced ECM production in renal fibroblasts, Int. J. Mol. Sci. 17 (2) (2016).
[16] Y. Shen, N.J. Miao, J.L. Xu, X.X. Gan, D. Xu, L. Zhou, et al., N-acetylcysteine alleviates angiotensin II-mediated renal fibrosis in mouse obstructed kidneys, Acta Pharmacol. Sin. 37 (5) (2016) 637–644.
[17] J.N. An, S.H. Yang, Y.C. Kim, J.H. Hwang, J.Y. Park, D.K. Kim, et al., Periostin induces kidney fibrosis after acute kidney injury via the p38 MAPK pathway, Am. J. Physiol. Renal. Physiol. 316 (3) (2019) F426–F437.
[18] P. Mundel, J. Reiser, W. Kriz, Induction of differentiation in cultured rat and human podocytes, J. Am. Soc. Nephrol. 8 (5) (1997) 697–705.
[19] S.H. Yang, J.W. Choi, D. Huh, H.A. Jo, S. Kim, C.S. Lim, et al., Roles of fluid shear stress and retinoic acid in the differentiation of primary cultured human podocytes, Exp. Cell Res. 354 (1) (2017) 48–56.
[20] K.J. Livak, T.D. Schmittgen, Analysis of relative gene expression data using real-time quantitative PCR and the 2(-Delta Delta C(T)) Method, Methods 25 (4) (2001) 402–408.
[21] C.V. Kavitha, M. Nambiar, C.S. Ananda Kumar, B. Choudhary, K. Muniyappa, K.S. Rangappa, et al., Novel derivatives of spirohydantoin induce growth inhibition followed by apoptosis in leukemia cells, Biochem. Pharmacol. 77 (3) (2009) 348–363.
[22] S.S. Han, M.Y. Yu, K.D. Yoo, J.P. Lee, D.K. Kim, Y.S. Kim, et al., Loss of KLF15 accelerates chronic podocyte injury, Int. J. Mol. Med. 42 (3) (2018) 1593–1602.
[23] A.M. el Nahas, A.H. Bassett, G.H. Cope, J.E. Le Carpentier, Role of growth hormone in the development of experimental renal scarring, Kidney Int. 40 (1) (1991) 29–34.
[24] S.H. Yang, J.P. Lee, H.R. Jang, R.H. Cha, S.S. Han, U.S. Jeon, et al., Sulfatide-reactive natural killer T cells abrogate ischemia-reperfusion injury, J. Am. Soc. Nephrol. 22 (7) (2011) 1305–1314.
[25] N. Li, J. Zhang, X. Yan, C. Zhang, H. Liu, X. Shan, et al., SIRT3-KLF15 signaling ameliorates kidney injury induced by hypertension, Oncotarget 8 (24) (2017) 39592–39604.
[26] G.S. Ceravolo, A.C. Montezano, M.T. Jordao, E.H. Akamine, T.J. Costa, A.P. Takano, et al., An interaction of renin-angiotensin and kallikrein-kinin systems contributes to vascular hypertrophy in angiotensin II-induced hypertension: in vivo and in vitro studies, PLoS One 9 (11) (2014) e111117.
[27] A.C. Stanley, K.M. Lounsbury, K. Corrow, P.W. Callas, R. Zhar, A.K. Howe, et al., Pressure elevation slows the fibroblast response to wound healing, J. Vasc. Surg. 42 (3) (2005) 546–551.
[28] M.W. Feinberg, Z. Lin, S. Fisch, M.K. Jain, An emerging role for Kruppel-like factors in vascular biology, Trends Cardiovasc. Med. 14 (6) (2004) 241–246.
[29] R. Pearson, J. Fleetwood, S. Eaton, M. Crossley, S. Bao, Kruppel-like transcription factors: a functional family, Int. J. Biochem. Cell Biol. 40 (10) (2008) 1996–2001.
[30] R. Malhotra, J. Sadoshima, F.C. Brosius 3rd, S. Izumo, Mechanical stretch and angiotensin II differentially upregulate the renin-angiotensin system in cardiac myocytes in vitro, Circ. Res. 85 (2) (1999) 137–146.
[31] B.M. Brenner, J.L. Troy, T.M. Daugharty, The dynamics of glomerular ultrafiltration in the rat, J. Clin. Investig. 50 (8) (1971) 1776–1780.
[32] I. Ishikawa, N.K. Hollenberg, Renal blood flow, afferent vascular resistance, and estimated glomerular capillary pressure in the nonexposed rat kidney, Circ. Res. 41 (1) (1977) 67–73.